Supporting Information

Gutiérrez-Medina et al. 10.1073/pnas.0907133106

SI Materials and Methods

Fluorescence Assay. The bead-based fluorescence assay for rotation offers the experimental advantage of lengthy observation times combined with comparatively high temporal and angular sensitivity. A high signal-to-noise ratio was achieved by using fluorescent markers permeated with multiple dyes. Useable photobleaching lifetimes were further extended by chopping the excitation light using an LCD-based shutter to expose the sample only during active video frame acquisition, and by slowly raising the illumination power during an experiment to compensate for any signal loss.

Dimeric Kinesin Bound to Microtubules (MTs) in Rigor. We induced a one-head-bound (1-HB) state for the kinesin dimer by attaching K448 to MTs in rigor, i.e., in the absence of exogenous nucleotides (residual [ATP] ~ 1 fM). The procedures for experiments under rigor conditions were the same as those under AMP-PNP conditions (see *Materials and Methods*), except that kinesin was incubated with beads for only 3 h at 4 °C, and no exogenous nucleotide was added. In rigor, we found that kinesin binds MTs in an admixture of attachment states (Fig. S2), biased toward 2-HB, but with a substantial minority in the 1-HB state, consistent with a previous report based on motor-detachment forces measured using an optical trap (1), and with a recent single-molecule fluorescence study that probed head location (2). Therefore, the rigor data reinforce the conclusion that the neck linker (NL) of the dimer acts as a free swivel.

Chemical Cross-Linking of Kinesin to MTs. Specific, covalent cross-linking between kinesin motor heads and MTs was performed stepwise using a "zero-length" coupling reagent to minimize the introduction of any undesired linkages (3–5). Taxol-stabilized MTs were first incubated in 50 μL of binding buffer (BB; 80 mM Pipes, pH 6.9/4 mM $MgCl_2$/1 mM EGTA/1.5 mM DTT/10 μM Taxol) with 2 mM 1-ethyl-3-[3-(dimethylamino)propyl]carbodiimide (EDC) and 5 mM *N*-hydroxysuccinimide (Sulfo-NHS) for 12 min at 22 °C. Next, 450 μL of BB was added and the total volume was transferred to a 10-kDa centrifuge filter (PALL) and spun at 12,000 rpm for 1 min, retaining ≈50 μL of volume. This step was repeated a total of three times, transferring to a different filter each time. After these washes (which took 10 min), we immediately added 50 μL of kinesin diluted in BB plus either 2 μM ATP or 2 mM AMP-PNP, then incubated 40 min at 22 °C. Motor-decorated MTs were immobilized on a polylysine-coated coverglass, and unbound motors were removed by several washes with an assay buffer containing ATP (2 mM). Last, fluorescently tagged beads were introduced, optically trapped, and held against a MT, then dragged along it longitudinally until a tether formed, pulling the bead from the trap. Cross-linking reactions were carried out in the presence of either 2 μM ATP or 2 mM AMP-PNP. Rotational assays on such motors were performed in the presence of a buffer containing ATP (2 mM), which further minimized the possibility that nonspecifically attached motors would remain bound to MTs. The kinesin concentration was adjusted during incubation so that a maximum of just two such binding events occurred along any given MT (≈10-μm length). The estimated probability of two or more motors binding simultaneously to a single bead was ≈1% or less.

Low Kinesin Detachment Rates. In all our data for stalled kinesin, the measured diffusional behavior persisted for hundreds of seconds, consistent with low spontaneous head detachment rates (<0.002 s^{-1}) under AMP-PNP or rigor conditions (6), or with stable cross-linking.

Running Variance. The running angular variance as a function of lag time was computed for each angle versus time record as follows. First, a time window of a particular size, τ, was defined. Then, the time window was positioned at the start of the record, defining the angle interval $\delta_0 = [\theta(t = 0), \theta(t = \tau)]$, and the variance was calculated over this same interval, yielding $\langle\delta(\tau)_0^2\rangle$. Next, the time window was advanced by Δ, the time between video frames, defining $\delta_1 = [\theta(t = \Delta), \theta(t = \tau + \Delta)]$, and the variance was calculated again, yielding $\langle\delta(\tau)_1^2\rangle$. This process was repeated until the interval $\delta_{T-\tau}$, where T is the duration of the record, and all $\langle\delta_i^2\rangle$ values were averaged to produce the variance associated with a particular lag time, τ, for a particular record: $\langle\delta(\tau)^2\rangle = [1/(T - \tau + 1)]\sum_{i=0}^{T-\tau}\langle\delta(\tau)_i^2\rangle$. Last, the ensemble-averaged variance $\langle\theta^2(\tau)\rangle$ was computed by averaging the $\langle\delta(\tau)^2\rangle$ values for all rotation records.

Stalk Reversals Absent in a Previous Experiment. Stalk reversals during processive kinesin motion were not reported in a previous experiment by the Gelles lab (7), which tested for MT rotation driven by K448-BCCP molecules at low ATP concentration using a gliding-filament assay. It seems possible that these reversals could have been present, but were missed because of their infrequency, but more likely, they may not have occurred due to differences in the experimental geometries. Among the salient differences are the following:

(*i*) The assay geometry: In our assay, the torsional relaxation time of a 1.3-μm bead tethered by a single K4EI molecule is τ_0 = 0.5 s, approximately comparable with the values reported for MTs tethered by K448-BCCP constructs in ref. 7. Also, the translational diffusion constant of a bead of radius r = 650 nm is $D_{bead} = k_BT/(6\pi\eta r) = 3.7 \times 10^5$ $nm^2{\cdot}s^{-1}$, also similar to that of MTs with length L = 2 μm and diameter d = 25 nm: $D_{MT} = \ln(L/d) \times k_BT/(4\pi\eta L) = 7.9 \times 10^5$ $nm^2{\cdot}s^{-1}$. However, these crude estimates do not take into account any corrections to the drag arising from surface proximity, which can be significant (Faxen's Law) (8). In this context, we note that in the gliding-filament assay, the MT is positioned extraordinarily close to the coverglass surface, separated by just the length of a kinesin molecule (≤30 nm) near its midpoint, and possibly even touching it near the MT ends. This tiny separation distance, and the diameter of the MT itself (≈25 nm), is comparable with the sizes of small aggregates of blocking proteins that are often present in the assays (such as BSA, used in ref. 7), and these aggregates may significantly affect otherwise free motions of MTs in solution, increasing the apparent relaxation time. Also, MT–surface electrostatic interactions that are present (9) may alter the damping properties of MTs. Any such surface effects are minimized in the bead-based assay.

(*ii*) The construct used for measurements: Differences between K448-BCCP and our K448-His tagged constructs are discussed in the main text. It is possible that the comparatively bulky C-terminal BCCP domain (87 aa, versus 6 His residues followed by one to four additional amino acids for the His tag) might interfere with large excursions of the MT in a surface assay, or with the mechanical properties of the kinesin stalk near its C terminus.

Stalk Reversals Cannot Be Explained Trivially by Both Heads Unbinding and Rebinding. The $\pm 180°$ rotations observed during processive kinesin motion cannot be explained by trivial mechanisms, such as the rapid, undetected unbinding and rebinding of both the kinesin heads (after a stalk reversal), as the following argument shows. Let M be the average number of steps taken per processive run. The average number of expected dissociation events as a function of N, the number of steps, is $n = N/M$. Assuming that all dissociation events are followed by rebinding events, and that all of these dissociation-rebinding events lead to either $+180°$ or $-180°$ stalk reversals (with equal probability), then the angular variance after N steps is $\langle \theta^2(N) \rangle = n \times (180°)^2 = N \times (180°)^2/M$. From the K4EI data at low ATP, we estimate $M \approx 80$, which implies a slope of variance versus N equal to $\Delta^2_{\text{estimate}} = (180°)^2/80 = 405°^2$, which is only 70% of the measured value, $\Delta_\theta{}^2 = 575°^2$. Also, this computation of variance is already a gross overestimate, because the stated assumptions are extreme. First, if all dissociation events were followed by rebinding events, we would have observed infinite processivity, which was not the case. In K4EI experiments at low ATP concentrations, we observed bead dissociation events (which defined the ends of records), and our estimates for the average run lengths were fully consistent with other measurements of unloaded kinesin moving on MTs (10). Second, the assumption that all dissociation-rebinding events lead to exactly $\pm 180°$ stalk reversals is unrealistic, because the molecule would not be expected to rotate at all in a significant fraction of the presumptive unbinding–rebinding events. Typical run lengths and the possibility of rebinding without stalk rotation would lead to a significantly lower value of $\Delta^2_{\text{estimate}}$, and therefore, to an even greater discrepancy with the observed value for the effective diffusion rate.

1. Uemura S, et al. (2002) Kinesin-microtubule binding depends on both nucleotide state and loading direction. *Proc Natl Acad Sci USA* 99:5977–5981.
2. Mori T, Vale RD, Tomishige M (2007) How kinesin waits between steps. *Nature* 450:750–754.
3. Song Y, Mandlekow E (1993) Recombinant kinesin motor domain binds to β-tubulin and decorates microtubules with a B surface lattice. *Proc Natl Acad Sci USA* 90:1671–1675.
4. Tucker C, Goldstein LSB (1997) Probing the kinesin-microtubule interaction. *J Biol Chem* 272:9481–9488.
5. Walker RA (1995) Ncd and kinesin motor domains interact with both α- and β-tubulin. *Proc Natl Acad Sci USA* 92:5960–5964.
6. Hancock WO, Howard J (1999) Kinesin's processivity results from mechanical and chemical coordination between the ATP hydrolysis cycles of the two motor domains. *Proc Natl Acad Sci USA* 96:13147–13152.
7. Hua W, Chung J, Gelles J (2002) Distinguishing inchworm and hand-over-hand processive kinesin movement by neck rotation measurements. *Science* 295:844–848.
8. Neuman KC, Block SM (2004) Optical trapping. *Rev Sci Instrum* 75:2787–2809.
9. Fordyce PM, Valentine MT, Block SM (2007) *Single-Molecule Techniques: A Laboratory Manual*, eds Selvin P, Ha T (Cold Spring Harbor Lab Press, Woodbury, NY), pp 431–460.
10. Thorn KS, Ubersax JA, Vale RD (2000) Engineering the Processive Run Length of the Kinesin Motor. *J Cell Biol* 151:1093–1100.

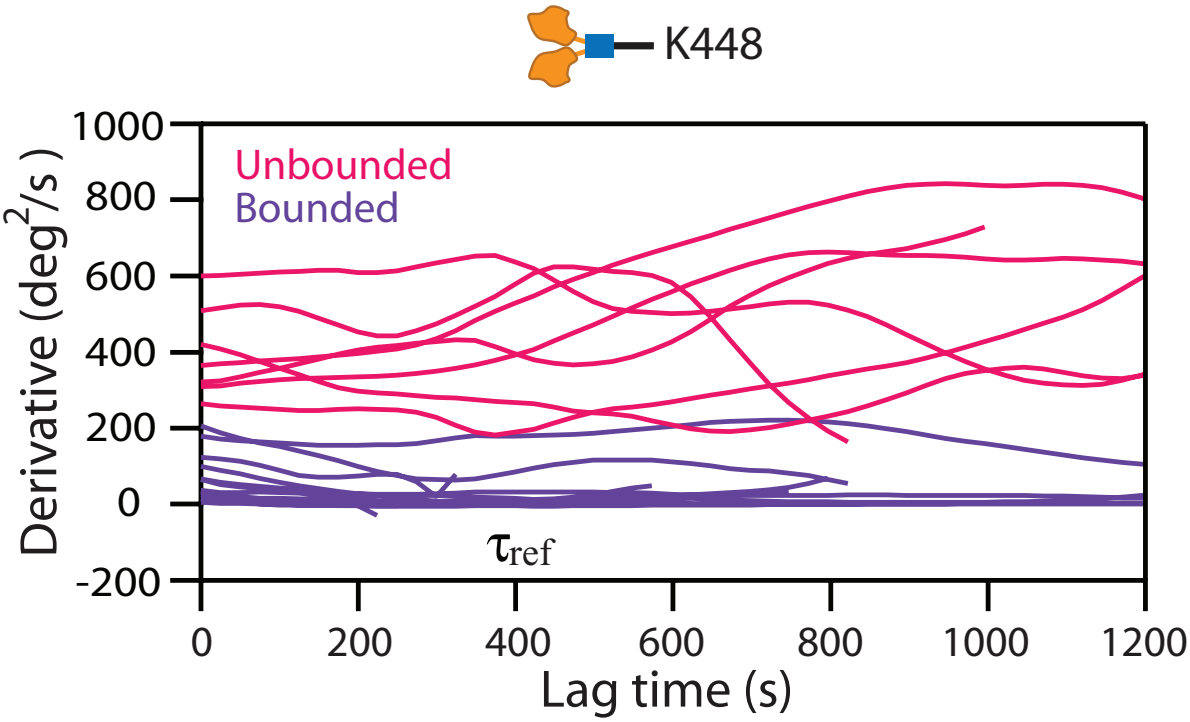

Fig. S1. Time derivative of the angular variance data displayed in Fig. 3*A*, for representative rotational records of K448 cross-linked to MTs in the presence of 2 μM ATP, producing an admixture of both 1- and 2-HB states. To separate individual records into ''unbounded'' and ''bounded'' groups, the variance time derivatives were calculated by finite differences from a fixed reference point ($\tau_{ref} = 400$ s), according to $\delta\theta = (\langle\theta^2(\tau)\rangle - \langle\theta^2(\tau_{ref})\rangle)/(\tau - \tau_{ref})$. Traces with derivatives converging toward zero were considered to be in the bounded group; traces whose derivatives fluctuated around a constant were classified as unbounded. All short traces ($t < 400$ s) were included in the bounded population.

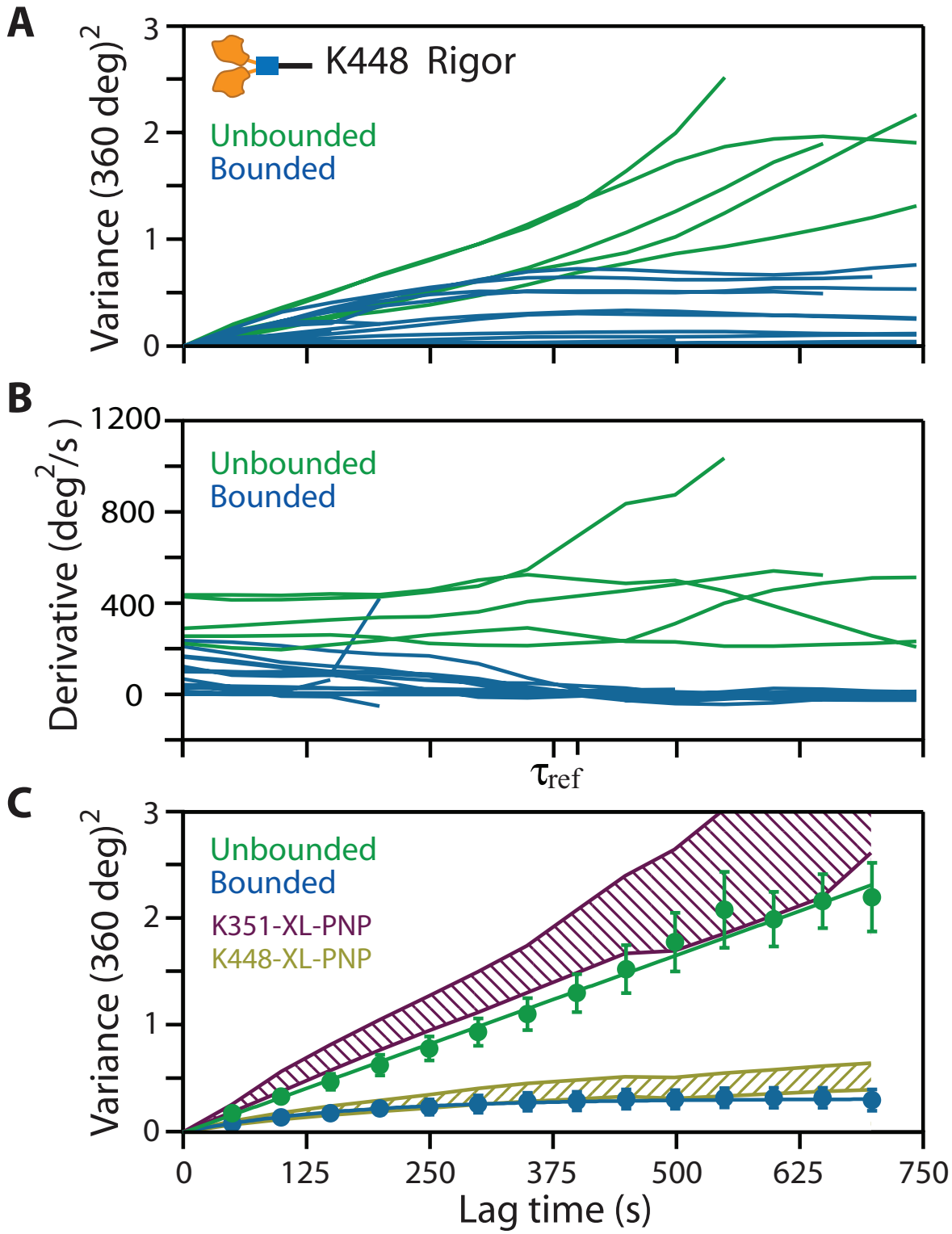

Fig. S2. Angular data for K448 in rigor revealed distinct subpopulations. (*A*) Individual records of the angular variance, colored according to behavior: unbounded diffusion (green, $N_u = 5$) and bounded diffusion (blue, $N_b = 18$). (*B*) Time derivatives of the data in *A*, using the same formalism as Fig. S1 ($\tau_{ref} = 400$ s), show traces that are asymptotically constant (green) or fall toward zero (blue). (*C*) Separate ensemble averages for the unbounded (green circles with SEs; fit to green line) and bounded (blue circles with SEs; fit to blue asymptotic curve) subpopulations were statistically consistent with data from control experiments representing the 1-HB state (K351-XL-PNP; purple hatched area) and 2-HB state (K448-XL-PNP; olive hatched area), respectively. The unbounded diffusion seen for a subset of K448-rigor rotation records confirms that the bound NL can act as a swivel. Fits to data (solid lines) were to free and constrained diffusion (see main text).

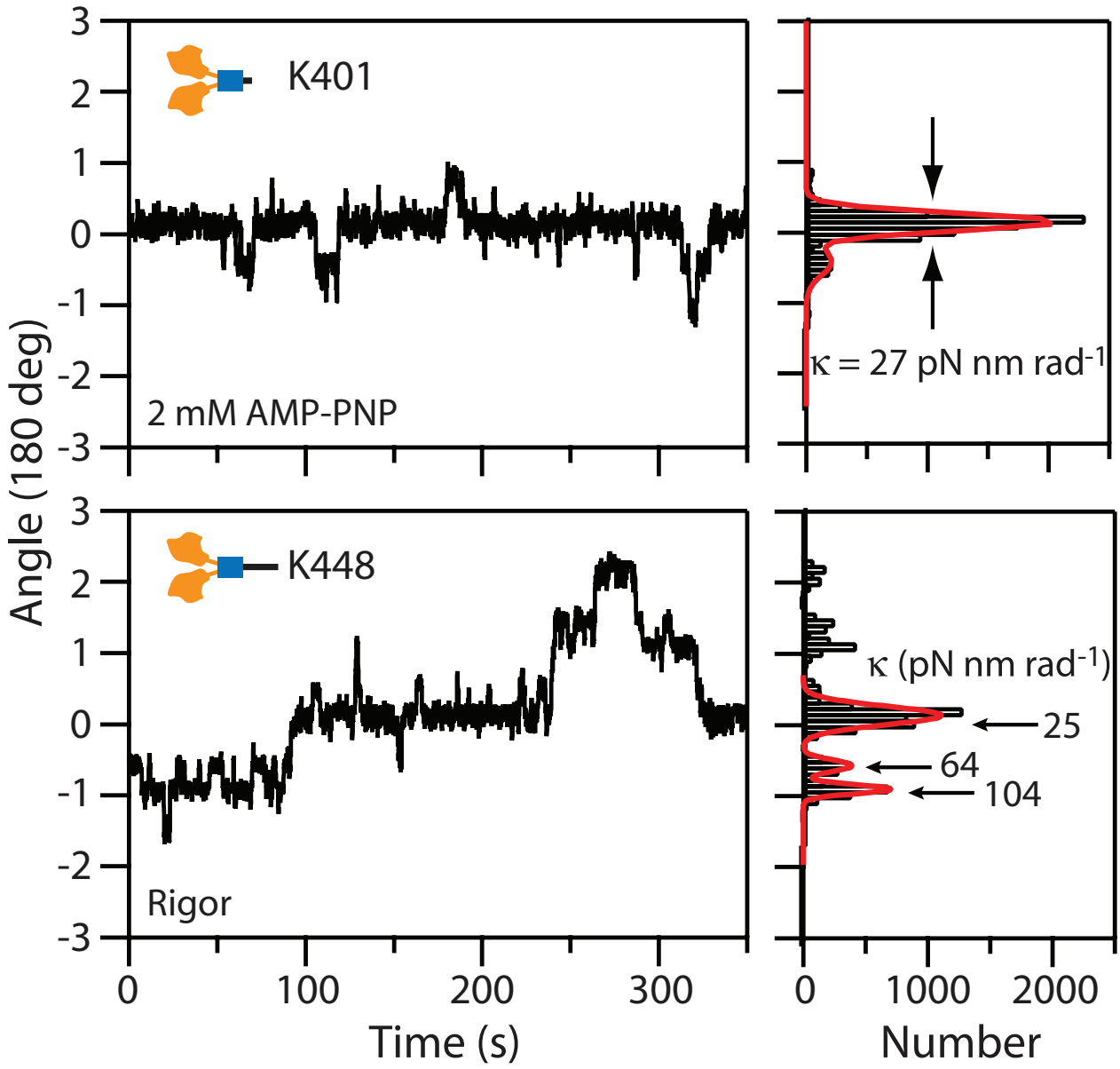

Fig. S3. A fraction of the kinesin rotation records for both K401 (*Upper*) and K448 (*Lower*) displayed distinct angular dwell states (*Left*), which appeared as well-defined peaks in the respective histograms of angle derived from these records (*Right*). The solid lines (red) show Gaussian fits to the histogram peaks, from which the associated torsional stiffness values (κ) were computed. We observed stable rotational states lasting up to tens of seconds in ≈50% of the records for K401 (2 mM AMP-PNP) and K448 (either cross-linked or in rigor). We did not observe such states for K4EI (2 mM AMP-PNP). Because of their relatively short durations (up to a few tens of seconds, compared with several hundreds of seconds for each complete angular record), and their limited angular dispersion (corresponding to high stiffness; $\kappa_{state} > 25$ pN·nm·rad^{-1}), the presence of these dwell states does not affect the global diffusive character of the molecule, nor the measured torsional stiffness values reported in our study, which were derived exclusively from the asymptotic variance of 2-HB records.

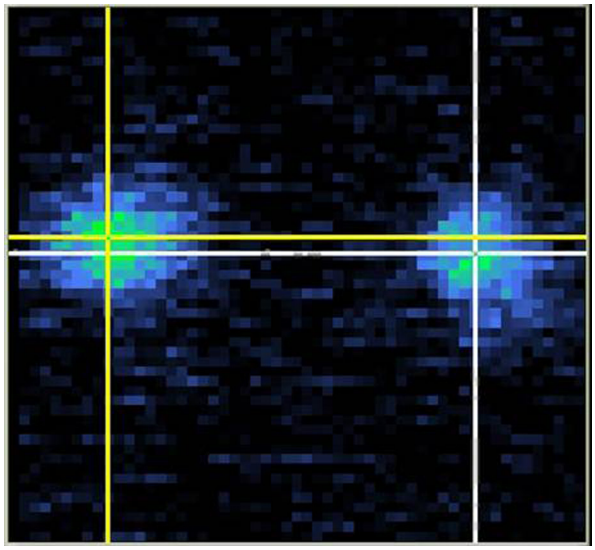

Movie S1. Real-time, false-color sequence of images displaying the angular motion of two fluorescent markers (green) attached to a larger, central bead tethered by a single recombinant kinesin molecule (K448) to an immobilized MT in the presence of AMP-PNP (2 mM). The central bead rotates at random with thermal energy about a mean angular position, with an rms amplitude directly related to the torsional compliance of the kinesin stalk. The superposed white and yellow crossed lines correspond to the centroid coordinates computed frame-by-frame for each of the two fluorescent markers. Field of view, 2.1 $\times$ 2.1 μm; camera frame rate, 33 fps.

Movie S1 (MOV)

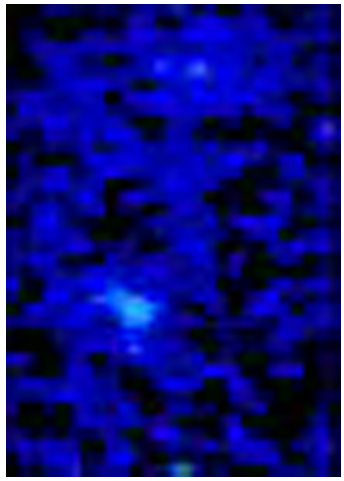

Movie S2. False-color sequence of images displaying the angular motion of two fluorescent markers (green) attached to a larger, central bead tethered by a single recombinant kinesin molecule (K4EI) walking along an immobilized MT in the presence of a low concentration of ATP (500 nM). The MT is oriented vertically in the image, with its plus end at the bottom. As the bead is transported by the motor, several abrupt reversals of its orientation can be observed, corresponding to $\pm 180°$ changes in the direction of the kinesin stalk. Field of view, 1.9×2.7 μm. The original sequence consisted of 10,900 frames, acquired at 21.8 frames per second. Here, to reduce file size, but at the cost of temporal resolution, only every fourth frame is displayed, and the playback rate has been increased $10\times$ for clarity (final rate, 54 frames per second). Total observation time, 500 s.

Movie S2 (MOV)